

Fabrication of Device Nanostructures Using Supercritical Fluids

Adam O'Neil and James J. Watkins

Abstract

Supercritical fluids including carbon dioxide offer a combination of properties that are uniquely suited for device fabrication at the nanoscale. Liquid-like densities, favorable transport properties, and the absence of surface tension enable solution-based processing in an environment that behaves much like a gas. These characteristics provide a means for extending "top-down" processing methods including metal deposition, cleaning, etching, and surface modification chemistries to the smallest device features. The interaction of carbon dioxide with polymeric materials also enables complete structural specification of nanostructured metal oxide films using a "bottom-up" approach in which deposition reactions are conducted within sacrificial, pre-organized templates diluted by the fluid. The result is high-fidelity replication of the template structure in a new material. In particular, block copolymer templates yield well-ordered porous silica and titania films containing spherical or vertically aligned pores that can serve as device substrates for applications in microelectronics, detection arrays, and energy conversion. Finally, the synthesis of nanoparticles and nanowires in supercritical fluids is developing rapidly and offers promise for the efficient production of well-defined materials. In this review, we summarize these developments and discuss their potential for next-generation device fabrication.

Keywords: block copolymer, mesoporous, metal deposition, nanoscale, polymer, supercritical fluid.

Introduction

Advancements in device technology, including those enabled by nanotechnology, will soon require the seamless integration of components and features with length scales ranging from nanometers to tens of micrometers on a common platform. While the most immediate example is the fabrication of next-generation processors and memory components using Si wafer technology, other applications, including the fabrication of high-performance sensors, photovoltaics, and optoelectronic devices, face similar challenges. Technical and economic constraints will favor the development of high-throughput "bottom-up" processing approaches for pattern and structure generation to define the smallest features. Once defined, the patterned

media will require subsequent metallization, deposition of adjacent layers, and other integration steps to create functional devices. At dimensions below 45 nm, current approaches are not fully capable of meeting these challenges.

In this review, we describe the use of supercritical fluids (SCFs) as a scalable process alternative to enable the fabrication of nanostructured devices. Although the primary focus is on device fabrication using Si wafer platforms, many of the techniques are relevant to materials processing needs in other fields including catalysis, energy conversion, and separation science. The properties of SCF media and the rationale for their use at the nanoscale are described first.

Next, SCF-enabled extensions of "top-down" deposition, etching, and cleaning techniques that can overcome existing limitations to device scaling beyond 45 nm are reviewed.

A discussion follows on the preparation of device substrates by the 3D replication of pre-organized polymer templates, a rapid and efficient bottom-up approach to well-defined metal oxide and carbon films, which provides complete specification of film structure and opportunities for direct patterning.

In combination, these approaches offer the potential for nanoscale device fabrication using a single platform; however, each can be integrated separately as required in existing Si wafer fabrication flows. We conclude with a brief discussion of nanoparticle and nanowire synthesis in SCFs, which offer promising routes to device components but will require hybrid integration strategies.

Supercritical Fluids as Processing Media for Nanostructured Devices

A supercritical fluid is simply a material heated and compressed beyond its critical temperature and pressure. Any substance heated beyond its critical temperature (T_c) cannot be liquefied, regardless of the pressure applied. By comparison, a vapor held below its critical temperature will condense at its vapor pressure, which is below its critical pressure (P_c). Carbon dioxide is the fluid of choice for many applications because it is nonflammable, nontoxic, and exhibits easily accessible critical parameters ($P_c = 7.38$ MPa, $T_c = 30.98^\circ\text{C}$); however, other fluids are used as specific requirements dictate (Table I).¹ As a gas is compressed above its critical point, it does not traverse a phase transition but rather exhibits a continuous increase in density. As shown in Figure 1a for carbon dioxide, density can be controlled through variations in system pressure and temperature and can meet or exceed that of liquid solvents.¹ Other physicochemical properties, including viscosity, are also pressure-dependent and generally intermediate to those of the liquid and gaseous states (Table II). A comparison of the surface tensions of water, hexane, and liquid CO_2 as a function of temperature at saturation is shown in Figure 1b.¹ At temperatures above the critical point, surface tension vanishes.

Liquid-like densities enable the dissolution of many organic and organometallic compounds in SCFs that can serve as precursors and reagents for subsequent processing steps. For example, Figure 1c shows the solubility of nickelocene in CO_2 at two temperatures as a function of den-

sity.² The combination of precursor and reagent solubility, favorable transport properties, and the absence of surface tension enables solution-based chemistry and processing in a supercritical medium that behaves much like a gas, providing a situation that is ideal for the fabrication of nanostructured components. For example, SCF-based deposition, etching, cleaning, and surface modification can be carried out within the smallest features without damage due to capillary forces, limitations to wetting or flow in confined geometries, or concerns about residual solvent con-

tamination. SCF processing can be considered a “dry” process, as the solvents dissipate completely upon depressurization. Moreover, transport in solution eliminates precursor and reagent volatility concerns that often prove to be limiting in vapor-phase processes.

The interaction of polymers with SCFs, particularly carbon dioxide, also provides unique opportunities for the preparation of nanostructured materials using a bottom-up approach, although for different reasons than those discussed for top-down processing. While most polymers

are insoluble in CO₂, pressure-mediated adjustments in density can be used to precisely control the dilation of polymers and the distribution of reactants between an insoluble polymer and the fluid media. The equilibrium-limited sorption of CO₂ in polystyrene and poly(*n*-butyl methacrylate) as a function of pressure and temperature is shown in Figure 1d.³ The sorption of modest amounts of the fluid can significantly increase the diffusivity of small molecules within the polymer,⁴ thereby enabling efficient reactions within the dilated polymer phase. As detailed later, deposition reactions within polymer templates diluted in CO₂ provide direct access to device-quality nanostructured silicate, titania, and carbon films.

Table I: Critical Parameters of Selected Solvent Systems.¹

Solvent	Critical Temperature (°C)	Critical Pressure (MPa)
Carbon dioxide	30.98	7.38
Ethane	32.18	4.87
Propane	96.68	4.25
Hexane	324.67	3.03
Water	373.95	22.06

Enabling Extensions of Top-Down Processes Using Supercritical Fluids

The fabrication of microelectronic devices using silicon wafer processing is currently conducted almost exclusively by top-down methods.⁵ The continuous drive to faster and higher-capacity processors and memory devices, as well as new media, requires practical access to smaller and smaller features. Integrated circuits with device features of 90 nm are currently in production, with 65-nm devices expected by 2007, 45 nm by 2010, and 32 nm by 2013.⁶ Realization of these goals requires not only advancements in lithography and device patterning, but also resolution of a number of other roadblock issues. One example is the deposition of metals within high-aspect-ratio structures for interconnect fabrication in integrated circuits and for electrode deposition in dynamic and ferroelectric memory applications. Another challenge remains in the preparation, treatment, and integration of porous ultralow-dielectric-constant films for interconnects. These films must be fabricated while simultaneously avoiding risks associated with feature and film damage caused by solvent infiltration or capillary forces during solvent removal. In recent years, the use of SCFs has been proposed as an enabling process alternative for semiconductor device fabrication.^{7–10} Here, we focus on processes that can overcome the limitations of current methods for the smallest device features.

Metallization and Etching

The deposition of metal films within high-aspect-ratio features is essential for the fabrication of interconnects, electrodes, and barriers for integrated devices. While vapor-phase techniques such as chemical vapor deposition are ideally suited for these applications in principle,

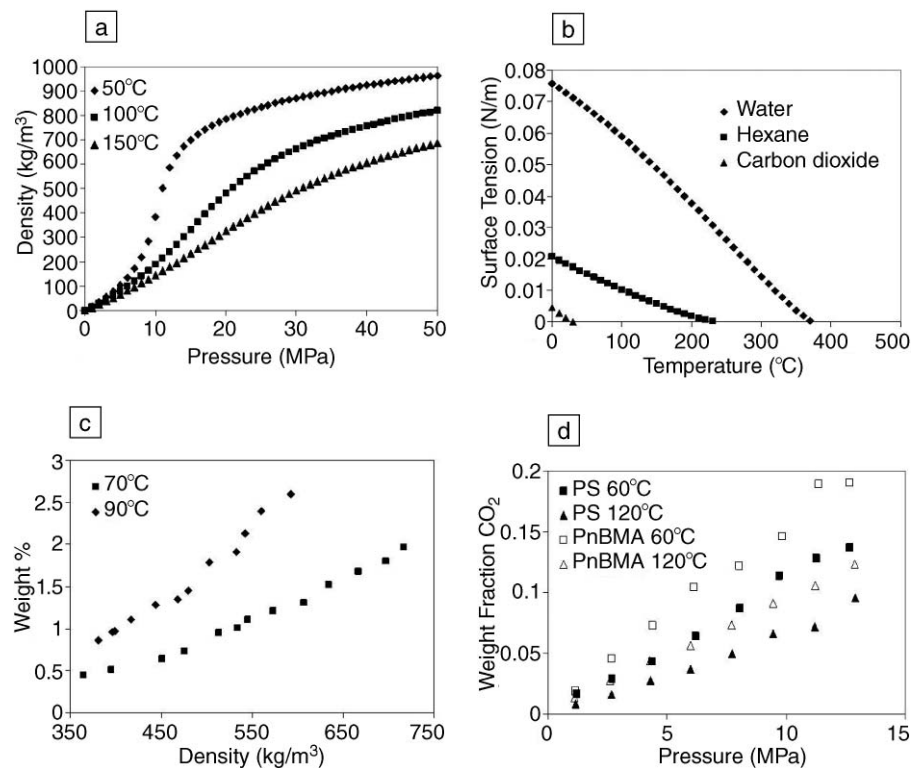


*Figure 1. Properties of supercritical fluid systems. (a) Density of CO₂ as a function of pressure for isotherms at 50°C, 100°C, and 150°C.¹ (b) Surface tension of water, hexane, and liquid carbon dioxide as a function of temperature at saturation. Surface tension for all fluids vanishes at the critical point.¹ (c) Solubility of nickelocene in supercritical CO₂ as a function of pressure at 70°C and 90°C.² (d) Solubility of CO₂ in polystyrene (PS) and poly(*n*-butyl methacrylate) (PnBMA) as a function of pressure at 60°C and 120°C.³*

Table II: Comparison of Selected Properties of Supercritical Fluids to Those of Liquids and Gases.

	Supercritical Fluid	Liquid	Gas
Density (g/cm ³)	0.1–1	1	10 ⁻³
Viscosity (Pa s)	10 ⁻⁴ –10 ⁻⁵	10 ⁻³	10 ⁻⁵
Diffusivity (cm ² /s)	10 ⁻³	10 ⁻⁵	10 ⁻¹
Surface Tension (dynes/cm)	0	20–50	0

their implementation has often been hindered by secondary issues such as precursor volatility, step coverage, film quality, and adhesion. For example, the difficulties associated with copper CVD prevented its commercialization for Cu interconnects, resulting in the current two-step approach consisting of Cu seed deposition by physical vapor deposition, followed by electrolytic plating.

Sievers and co-workers were among the first to use SCFs in connection with precursor volatility in CVD processes.^{11,12} In their work, precursor aerosols were produced by preparing solutions of precursors in a supercritical fluid, followed by rapid expansion of the supercritical solvent (RESS) to atmospheric pressure upstream of a CVD reactor. The aerosol was directed at a substrate to produce a film at elevated temperatures (500–800°C). The process, called supercritical fluid transport and chemical deposition (SFT-CD), was used to produce films of Al, Ag, Cr, Cu, In, Ni, Pd, Y, and Zr. A variant of SFT-CD was used to produce metal oxide films by expansion from solutions in N₂O, a strong oxidizing agent, into a high-energy plasma. This technique has allowed the generation of Al₂O₃, Cr₂O₃, CuO, SiO₂, and B-doped and P-doped SiO₂, although the use of N₂O requires extreme care.¹¹ Popov et al. used a similar method to generate InP films.¹³ While these approaches offer a useful means of generating aerosols of low-volatility precursors, deposition and film formation occurs at conditions similar to those of CVD and therefore does not overcome issues related to poor step coverage in confined geometries.

Recently, we and others have demonstrated the deposition of uniform metal films over very challenging topographies by carrying out reactive depositions using a process called supercritical fluid deposition (SFD).¹⁴ SFD involves the deposition of metals and metal oxide films by reaction of suitable precursors in an SCF solution at a heated surface within a high-pressure deposition reactor. Typical precursors include metallocenes and metal diketonates. Many common CVD precursors are sufficiently soluble in CO₂ and provide a suitable starting point for

screening potential chemistries. Reduction of the metal deposition precursor is commonly performed using hydrogen or alcohol,¹⁵ which are miscible with supercritical CO₂ above the mixture critical points. This approach has been used for the deposition of high-purity metal films including Au, Co, Cu, Ir, Ni, Pd, Pt, Rh, and Ru.^{16–22} The use of a cold-wall pressure vessel, in which the substrate is mounted on a heated stage, provides a means to localize the deposition to the desired surface.

The high precursor concentrations accessible in SFD promote conformal coverage (Figure 2). The deposition of copper by hydrogen reduction of Cu(II) β-diketonates including 2,2,6,6-tetramethyl-3,5-heptanedionato copper is well suited for the preparation of copper interconnects (Figure 2a).¹⁴ Cu depositions are typically carried out at pressures between 10 and 25 MPa and substrate temperatures between 200°C and 300°C. At temperatures above 225°C, seed layers are not required on dielectric or barrier surfaces, yielding a single-step method for feature fill. A kinetic analysis of the copper deposition process was performed by Zong et al. and revealed a zero-order reaction-rate dependence on precursor concentration for all but the most dilute reaction conditions (Figure 2b).²³ The ability to maintain zero-order kinetics over a large range of concentrations facilitates exceptional step coverage, as concentration gradients that may arise in the trench are insufficient to cause a transition out of the surface reaction-rate-limited regime. Thus, the reaction proceeds conformally over all surfaces, provided that the temperature is uniform. Simple substrate pre-treatments have been shown to yield good adhesion for Cu films deposited from CO₂.²⁴

Thin ruthenium films are of interest for use as both barriers and capacitor electrodes and can also be deposited with exceptional step coverage using SFD. For example, Kondoh demonstrated defect-free filling of high-aspect-ratio 100-nm-wide features on seeded Si wafers by the hydrogen reduction of ruthenocene (Figure 2c).²² We have deposited continuous and conformal films

as thin as 20 nm directly within high-aspect-ratio via structures by hydrogen reduction using chemistry that does not require a seed layer.²¹ Interestingly, H₂ reductions of Ru precursors proceed readily in CO₂ to yield high-purity films. This is typically not the case in CVD, where deposition under oxidizing conditions is more common and can lead to oxygen and carbon contamination that is deleterious to device performance.

Work has also been carried out using the codeposition of multiple precursors to form films containing a mixture of materials.^{25,26} For example, phosphorus-doped metal films [Co(P)] can be prepared by the reduction of 2,2,6,6-tetramethyl-3,5-heptanedionato cobalt in the presence of triphenylphosphine, and Pt/Ni alloyed films of tailored composition can be produced by coreduction of dimethylcyclooctadiene platinum and nickelocene with H₂ in CO₂.^{25,26} By operating at temperatures from 275°C to 325°C, the Co(P) films could be deposited on Cu lines selectively over the surrounding dielectric, providing an efficient means of Cu line capping.²⁵ In a variant of the alloy strategies, the deposition temperature of Cu and Ni films can be significantly reduced by the reduction of their precursors in the presence of trace quantities of easily reducible Pt or Pd compounds.^{14,26–28}

Cabanas et al. have demonstrated the preparation of patterned metal films templated by an underlying substrate.²⁰ Gold was deposited within high-aspect-ratio vias that were etched in Si and backfilled with a thin layer of SiO₂. The gold film was then released from the substrate by etching the underlying oxide with HF, yielding an array of high-aspect-ratio gold posts (Figure 2d).

Alternative deposition strategies have also been developed. Ye et al. deposited Cu, Ag, and Pd onto Si and Ge using HF as a reacting agent to facilitate deposition on Si and Ge surfaces.²⁹ The fluorination of semiconductor surfaces initiates reduction of the precursor to yield conformal metal films. Wakayama et al. have taken advantage of the excellent transport properties of SCF solutions to prepare freestanding metal and metal oxide nanostructured materials by permeating and coating solid porous materials such as activated carbon and woven carbon templates in carbon dioxide.³⁰ While the resulting materials are not relevant to the fabrication of semiconductor devices, the process is an excellent illustration of the ability of SCF media to deliver conformal coverage in confined geometries.

Device manufacture requires the removal of metals and metal oxides by etch-

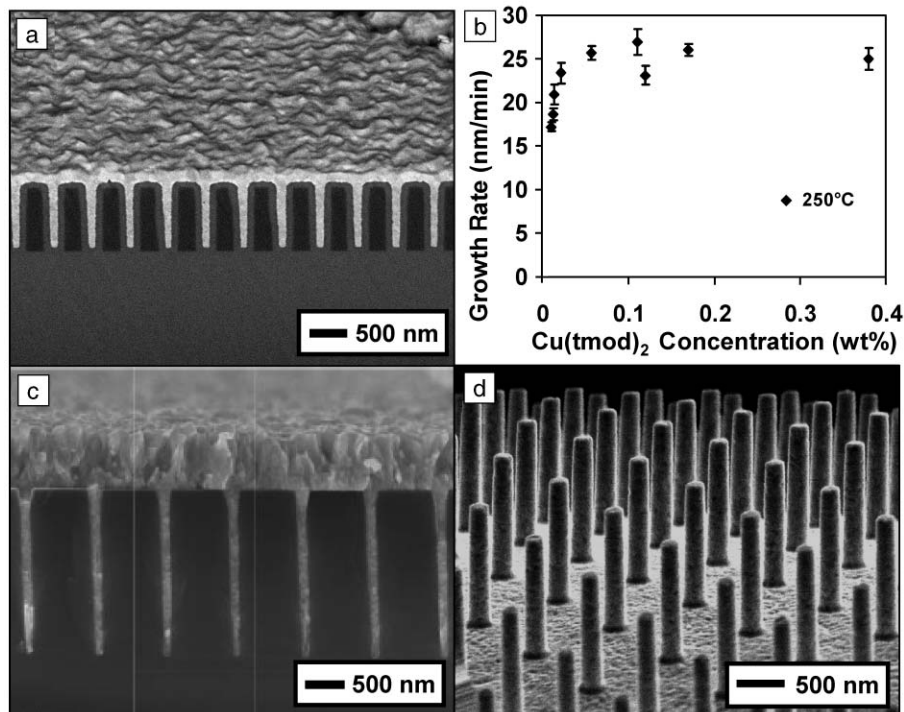


Figure 2. Metal deposition in supercritical carbon dioxide. (a) Cu deposited within high-aspect-ratio trench structures by the hydrogen reduction of bis-2,2,6,6-tetramethyl-3,5-heptanedionato copper [Cu(tmhd)₂] in supercritical carbon dioxide. Image reproduced with permission from Reference 14. (b) Film growth rate dependence on precursor concentration for Cu depositions by hydrogen reduction of bis-2,2,7-trimethyl-3,5-octanedionato copper [Cu(tmhd)₂] in supercritical carbon dioxide. Zero-order dependence of growth rate over a broad precursor concentration range promotes excellent step coverage.²³ (c) Conformal Ru film deposited within a trench structure deposited by the H₂ reduction of ruthenocene in supercritical carbon dioxide. (Image courtesy of E. Kondoh.) (d) Self-supporting arrays of gold posts prepared by the hydrogen-assisted reduction of (acac)Au(CH₃)₂ in CO₂ solution within high-aspect-ratio vias after release from the template. Used with permission from Reference 20.

ing for contamination control and for pattern generation via anisotropic etch processes. In many cases, dry etching is limited by either the volatility of the etching agents or resulting metal chelate or halide by-products. For example, anisotropic Cu metal etching is limited by the volatility of Cu halides.³¹ Rather than dry etching, the current dual damascene process for the fabrication of Cu interconnects relies on chemical-mechanical planarization to remove excess copper after electroless deposition. As with SCF deposition processes, a supercritical fluid can be used to overcome species volatility constraints for dry etching. DeSimone and co-workers demonstrated the etching of Cu in supercritical carbon dioxide using solutions of organic peroxides and hexafluoroacetylacetone (hfacH) free ligand, where the terminal H indicates the protonated form of the ligand.³² Here, the peroxides are necessary to oxidize the copper. The Cu oxides can then be etched using hfacH as the chelating agent, resulting in removal of the

metal film. Xie et al. conducted a detailed study of the etching of copper by sequential oxidation at ambient conditions followed by exposure to hfacH in supercritical CO₂.³¹ Shan and Watkins studied the etching kinetics of cuprous oxide films (Cu₂O) supported on Cu or on SiO₂ using several β-diketones including hfacH, 2,2,6,6-tetramethyl-3,5-heptanedione (tmhdH) and 2,2,7-trimethyloctane-3,5-dione (tmodH) in supercritical carbon dioxide at temperatures between 80°C and 150°C and pressures between 20 MPa and 27.5 MPa.³³ At 150°C, the etch rate using tmodH was 1.5 nm/min. Based on the activation energy obtained from the studies (65 kJ/mol), etch rates greater than 10 nm/min can be obtained at 200°C. Carrying out the etching chemistry in SCF CO₂ enables the use of non-fluorinated chelating agents such as tmhdH and tmodH, which reduces fluorine contamination in the films and lessens environmental, health, and safety concerns.

Surface Modification of Nanoporous Substrates

The low viscosity, absence of surface tension, and ease of removal of supercritical solutions render them ideal vehicles for carrying out chemistry on and within nanoporous solids. Future generations of semiconductor devices are expected to employ silicate-based ultralow-dielectric-constant films with significant volume fractions of sub-3-nm pores. The groups of Tripp and McCarthy have demonstrated that CO₂ is an excellent medium for surface modification via silylation chemistry.^{34,35} Recent work by Muscat and Reidy have demonstrated that these chemistries can be adopted for the efficient surface modification of porous low-κ materials.^{36–38} For example, Xie et al. demonstrated that silylation of porous methylsilsequioxane thin films using hexamethyldisilazane or trimethylchlorosilane significantly increased the hydrophobicity of the films, effectively repairing damage that occurred during exposure to oxygen ashing used in photoresist removal.³⁸

Drying, Cleaning, and Photoresist Processing

Supercritical drying has been widely applied to nanostructured materials and devices including aerogels and microelectromechanical systems to avoid damage that can occur by capillary forces during the removal of liquid solvents. The field is well reviewed elsewhere¹⁰ and will not be broadly discussed, but a few examples relevant to device manufacturing are highlighted here. Goldfarb et al. used a CO₂/hexane/surfactant system to dry high-aspect-ratio resist patterns without feature collapse.^{39–41} The resist lines were 140 nm thick, with a spacing of 370 nm and aspect ratio of 6.8.³⁸ Conventional drying of these structures when rewetted with water and hexane led to structural collapse. Namatsu et al. demonstrated solvent removal from 7-nm resist features with an aspect ratio of 10, also using a surfactant, and recently used water displacement with SF₆ followed by supercritical removal to effectively dry surfaces without damage (Figure 3).^{42–44}

CO₂ has also been used for both spin-coating⁴⁵ and the direct development of photoresists. Ober et al. demonstrated the direct development of negative-tone resists comprised of copolymers of tetrahydropyranyl methacrylate and fluorinated methacrylates in which acid cleavage of exposed tetrahydropyranyl groups rendered a solubility difference sufficient for CO₂ development.⁴⁶ More recently, Ober modified this system to provide a high-

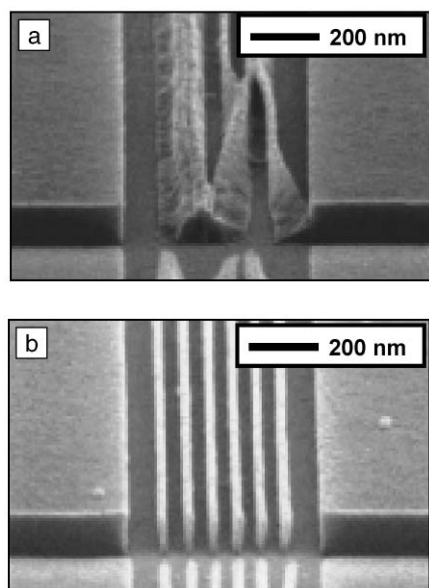


Figure 3. Photoresist drying in supercritical fluids. (a) Scanning electron microscopy (SEM) image showing damage to an acrylate resin resist pattern after conventional N_2 drying. (b) SEM image showing results of drying by supercritical-phase solvent removal. Images reproduced with permission from Reference 44.

resolution positive-tone resist that could be developed in CO_2 (see the article by Ober et al. in this issue).⁴⁷ Resist systems for CO_2 development have also been reported by DeSimone's group.⁴⁸

A Bottom-Up Approach to the Preparation of Nanostructured Metal Oxide and Carbon Films as Device Substrates

The ability to produce substrates with features below 45 nm and well-ordered metal oxide or carbon films with nanometer-scale periodic structures is es-

essential for the continued scaling of micro-electronic devices including processors and memory, and for the development of next-generation devices for applications in sensing and detection arrays, energy conversion and storage catalysis, separations, microfluidics, and other areas. The prohibitive cost and technical difficulty of lithographic patterning of device substrates below 45 nm is well documented. For applications requiring nanoporous or two- and three-dimensional periodic metal oxide or carbon structures, additional challenges exist. These include the ability to form dimensionally stable, defect-free films of tailored composition over large areas, and the ability to precisely control length scales, order, and orientation in the pore or feature structure.

While realization of complete control of these issues for metal oxide films has proven to be very difficult, preparation of the analogous structures in polymers is now in hand. Articles in this issue by the groups of Hawker and Russell, Willson, and Ober demonstrate tremendous progress in the complete specification of polymer nanostructures using high-throughput techniques including block copolymer assembly, nanoimprint lithography, and two-photon lithography. The use of supercritical fluids provides a direct route for high-fidelity replication of these structures in metal oxide and carbon films in three dimensions.

Block copolymers (BCPs) are nearly ideal templates for nanostructured materials. They consist of two or more polymer segments that are covalently bonded together and can self-assemble into ordered arrays of microdomains having dimensions on the order of 5–100 nm.⁴⁹ The size, shape, and spacing of the domains can be controlled by adjusting composition (block volume fraction) and block length. Moreover, BCP films can be processed over broad areas on Si wafers using processes amenable to high-volume manufacturing.

Recent advances have demonstrated unprecedented opportunities for controlling order and domain orientation using controlled solvent evaporation and topological constraints. A complete review of these advances is provided by Hawker and Russell in this issue.

The interaction of polymers with supercritical fluids enables the replication of polymer nanostructures by phase-selective deposition reactions within the templates. Most polymers are insoluble in CO_2 , but can be swollen by fluid sorption at modest temperatures and pressures. This sorption is equilibrium-limited and can be precisely controlled (Figure 1d). In block copolymers, sorption of modest amounts of SCFs does not disrupt microphase segregation (see the articles by Yang et al. and by Stewart and Wilson in this issue of *MRS Bulletin*).^{50,51}

In fact, annealing in supercritical CO_2 can relieve kinetic constraints for producing well-ordered films of high-molecular-weight block copolymers⁵² by increasing chain mobility.⁵³ Modest mass uptakes of CO_2 can dramatically increase the mobility of small molecules within the dilated polymers⁴ by depressing glass-transition temperatures.⁵⁴ Consequently, SCF-dilated polymer films are good reaction media. This fact has been exploited for the preparation of novel polymer blends by *in situ* polymerization of monomers^{55–57} and the preparation of metal nanoparticles within polymer substrates by the sequential in-fusion and reduction of organometallic compounds.⁵⁸ Confinement of deposition reactions within one phase of a dilated block copolymer provides an opportunity to use these materials as templates.

The replication of block copolymer template films diluted with supercritical carbon dioxide for the preparation of device-quality silica films has been demonstrated by Watkins and co-workers.⁵⁹ A diagram of the replication scheme is shown in Figure 4.

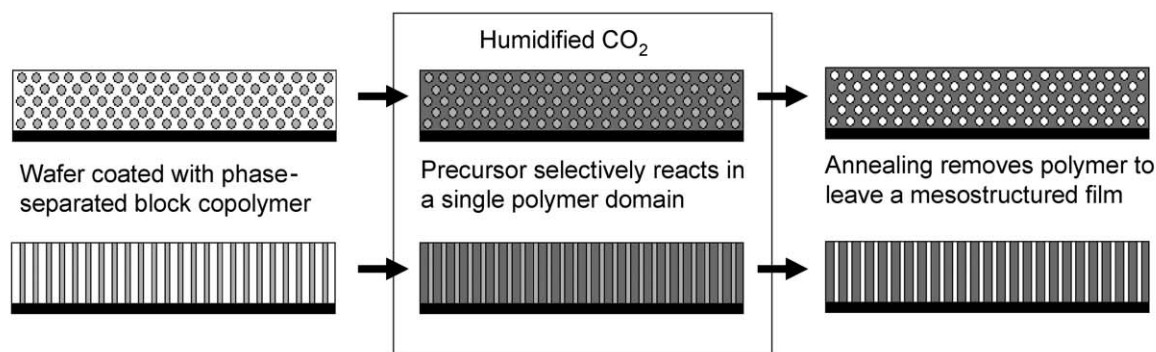


Figure 4. Schematic illustration of the process for 3D replication of block copolymer templates in supercritical CO_2 .

The process is straightforward and involves spin-coating a suitable template onto a support, transferring the template to a high-pressure reactor for SCF-assisted infusion and deposition within the template, and removal of the template following decompression by calcination, reactive plasma, or other techniques. The key to the process is imparting selectivity for the deposition reaction during the infusion, which can be achieved by localizing a catalyst within the polymer template.

Figures 5a and 5b show scanning electron microscopy cross sections of silica films prepared using this approach. In these examples, poly(ethylene oxide)-poly(propylene oxide)-poly(ethylene oxide) (PEO-*b*-PPO-*b*-PEO) triblock copolymer surfactants known commercially as Pluronics were used as templates and were spin-coated onto Si wafers from ethanol solutions containing *p*-toluene sulfonic acid (pTSA).⁵⁹ Upon solvent evaporation, the block copolymer microphase-separates to yield an ordered morphology, and the pTSA segregates to the hydrophilic PEO block of the copolymer. The silica films are then prepared by exposure of the templates to solutions of tetraethyl orthosilicate (TEOS) in humidified CO₂. During infusion of the template, silica condensation occurs only in the PEO domains of the template, which contains the pTSA catalyst. No condensation occurs in the SCF phase, as the catalyst is insoluble in CO₂. Following depressurization, template removal by calcination yields the silica replica. A high degree of order is evident in the films.

In Figure 5a, the random orientation of grains with a cylindrical pore structure in the silica is analogous to grain structure observed in unoriented films for cylindrical diblock copolymers. Orientation of cylindrical domains normal to a substrate prior to alkoxide infusion should provide access to nanochannel arrays in metal oxides. This has now been realized by the infusion of TEOS into cylindrical poly(α -methylstyrene)-*b*-poly(hydroxystyrene), PMS-*b*-PHOST copolymer templates,⁶⁰ which orient spontaneously upon spin-coating from propylene glycol methyl ether acetate.⁶¹ The resulting film is shown in Figure 5c. The diameter of the channels can be adjusted easily by using copolymers of varying molecular weight.

The composition of the metal oxide films prepared by this approach can be tuned by selection of the metal alkoxides. Infusion of BCP templates with mixtures of TEOS and methyltriethoxysilane (MTES) yields robust, ordered, mesoporous organosilicate films that are exceptional candi-

dates for use as ultralow-dielectric-constant thin films for microelectronics. The mechanical and electrical properties of films containing spherical pores can be tuned

by adjustments in alkoxide precursor mixtures and by adjustments in the mass uptake of silicate in the polymer templates during infusion. Defect-free uniform films

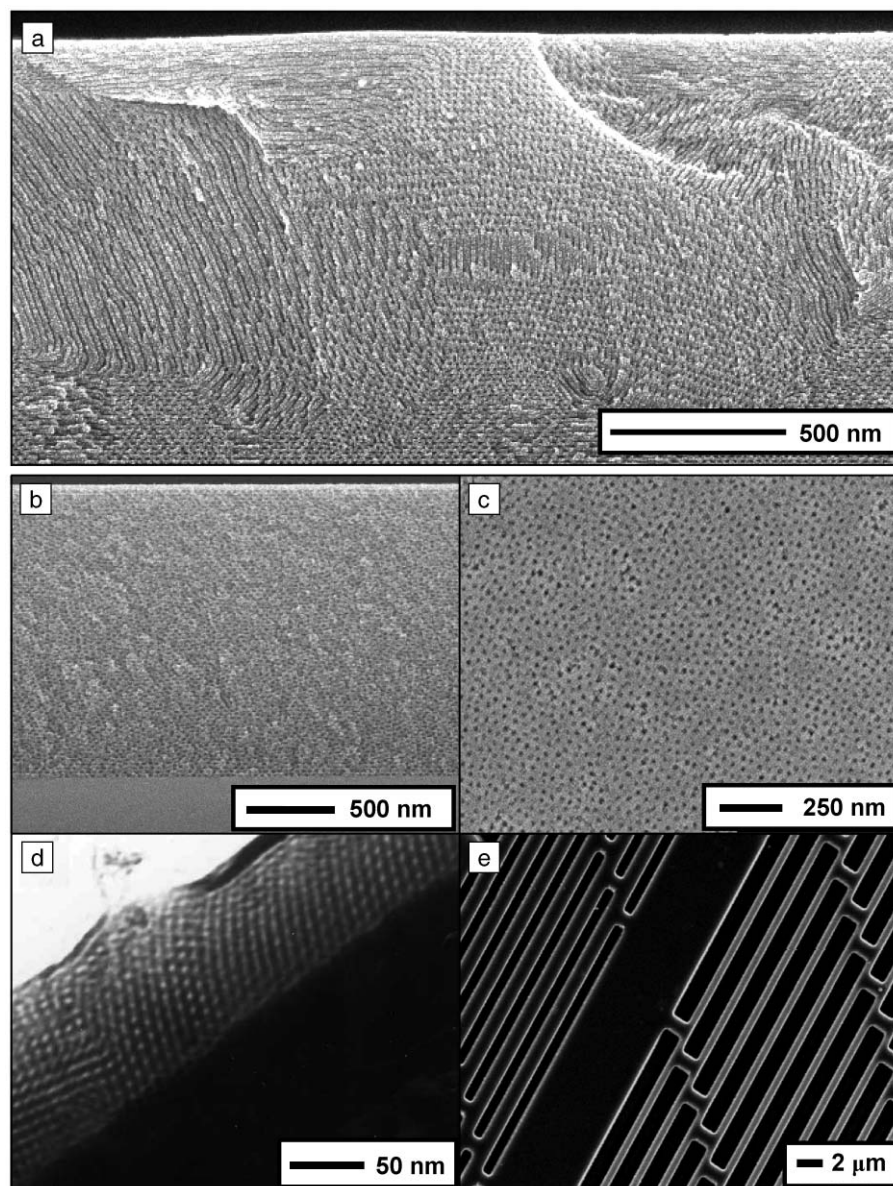


Figure 5. Nanostructured metal oxide films prepared by 3D replication of block copolymer templates in supercritical CO₂. (a),(b) Scanning electron microscopy (SEM) images showing the cross sections of highly ordered mesoporous silica films prepared on Si wafers by the infusion and condensation of tetraethyl orthosilicate (TEOS) within pre-organized PEO₁₀₆-*b*-PPO₇₀-*b*-PEO₁₀₆ and PEO₁₂₇-*b*-PPO₄₈-*b*-PEO₁₂₇ films, respectively, followed by removal of the template. Infusion conditions in supercritical CO₂ were 60°C and 12.3 MPa.⁵⁹ (c) Top-down SEM image of vertical nanochannels in a silica array prepared by TEOS infusion within an oriented cylindrical poly(α -methylstyrene)-*b*-poly(hydroxystyrene) block copolymer template.⁶⁰ (d) Transmission electron microscopy (TEM) image of a mesoporous titania film prepared by supercritical CO₂-assisted infusion and condensation of infusion titanium diisopropoxide bisacetylacetonate within a block copolymer template blend.⁶⁶ (e) SEM image of a patterned porous carbon film. The film was prepared by infusion and polymerization of furfuryl alcohol within a *p*-toluene sulfonic acid (pTSA)-doped block copolymer template cast onto a patterned silicon wafer followed by carbonization. The pattern was effectively transferred from the Si wafer to the freestanding carbon film.

prepared on 200-mm wafers exhibiting a dielectric constant of 2.2 were metallized with copper and shown to withstand the rigors of chemical–mechanical planarization, a crucial test required for device integration.⁵⁹ A detailed study of the pore structure in the film indicated a substantial fraction of microporosity in the pore walls, which contributes to the low dielectric constant without unduly compromising film strength.⁶² It is important to point out that the low- κ films can be prepared on full process wafers with good uniformity and short cycle times, which are vital for successful implementation.

Recently, Pai extended the scope of the technique by the fabrication of mesoporous silicate films using bridged silsesquioxanes including bis(triethoxysilyl)ethane, bis(triethoxysilyl)methane, and bis(triethoxysilyl)ethylene, and the functionalization of the interior pores of porous silicate films prepared by this templating technique by post-synthesis reaction with silane coupling agents in CO₂.⁶³

Porous titania films are of interest for applications including solar cells, sensors, and optoelectronics. One advantage of the SCF process for titania is the inherent use of a nonaqueous solvent system; most titanium alkoxides are hydrolytically unstable and difficult to handle in traditional aqueous sol-gel strategies.⁶⁴ Figure 5d shows a transmission electron micrograph of a porous titanium film prepared by infusion of titanium diisopropoxide bisacetylacetonate (TDIAC) into a template comprising a blend of Pluronic F108 and poly(vinyl phenol) ($M_w = 20,000$) spin-coated from a solution containing pTSA.⁶⁵ Here, the pTSA is necessary to promote complete hydrolysis and condensation of the TDIAC.

While up to now studies have focused on the replication of morphologies presented by block copolymers, there are no apparent barriers to extending SCF-assisted infusion strategy to polymer templates defined by other methodologies, including nanoimprint lithography or simple pattern transfer methods. Such an approach would provide broad and direct access to metal oxide and other films with arbitrary nanoscale patterns. A simple example at larger length scales is provided in Figure 5e, which shows a patterned carbon film prepared by infusion and polymerization of furfuryl alcohol within a pTSA-doped block copolymer template cast onto a patterned silicon wafer. After carbonization to remove the template, the resulting carbon film was removed from the wafer by an acid etch. The wafer pattern was effectively transferred to the carbon film with exceptional fidelity.⁶⁶

Efficient Production of Nanoparticles and Nanowires

Metal and semiconductor nanowires and nanoparticles are of interest for numerous optical and electronic devices. Once integration issues are resolved, these materials could yield significant enhancements in displays, solid-state lighting, memory devices, and medical diagnostics.⁶⁷ Supercritical fluids are versatile media offering potential advantages in the areas of particle size control, product recovery, and high-temperature synthesis. Synthetic strategies include direct reaction in supercritical solution, reaction in water-in-fluid reverse micelles, and seeded growth in high-temperature alkanes.

Shah et al. prepared nanoparticles of silver, iridium, and platinum in supercritical carbon dioxide by chemical reduction of appropriate precursors in the presence of capping ligands such as dodecane thiol for supercritical hydrocarbons and perfluorodecane thiol for carbon dioxide.⁶⁷ The capping ligands mediate growth and aggregation of the incipient particles. The technique, called arrested precipitation, has also been extended for the preparation of Si and Ge particles by the thermal decomposition of precursors such as diphenylsilane in supercritical hexane using octanol as the capping ligand at high temperatures (450°C). Particles produced by this process exhibit high core crystallinity and superior chemical stability relative to particles grown at lower temperature in conventional solvents. The high critical temperature of hexane is advantageous, as operation at modest pressure provides sufficient solvent densities to maintain high capping ligand concentrations, thus maximizing yield.

Nanoparticles can also be produced by the reduction of metal precursors within water-in-fluid reverse micelles. Water micelles in CO₂ are most commonly stabilized by fluorinated surfactants and give rise to discrete particles including silver, copper, CdS, and ZnS.^{68–71} Coordination of the surfactant with the growing particle stabilizes the system and prevents aggregation. Kitchens et al. used water-in-supercritical alkane reverse micelles to generate copper nanoparticles (Figure 6).⁷⁰ Sodium bis(2-ethylhexyl) sulfosuccinate (AOT) was used both as the surfactant molecule and as the capping ligand for stabilizing the copper particles. The mean particle size in propane was found to be a function of solvent density, increasing from 5.4 nm to 9 nm as pressure was increased from 24.1 MPa to 34.5 MPa.⁷⁰ McLeod et al. recently demonstrated improved particle size selectivity by preparing a surfactant-stabilized hexane dispersion

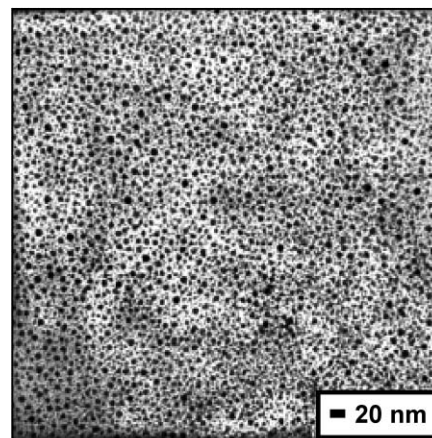


Figure 6. Preparation of copper nanoparticles in supercritical fluid: transmission electron microscopy image of copper nanoparticles synthesized in a propane-sodium bis(2-ethylhexyl) sulfosuccinate (AOT) reverse micelle system. Reproduced with permission from Reference 73.

of previously prepared particles and performing sequential pressurization of the solution with CO₂ to reduce the solvent strength and precipitate the particles.⁷² This was carried out in a tubular reactor containing a spiral screw, permitting the isolation of a narrow size distribution of particles through stepwise expansion of the solvent.

Semiconductor nanowires offer interesting prospects for logic gates, nanolasers, photodetectors, and memory devices.⁷³ Bulk quantities of single-crystal silicon and germanium nanowires have been synthesized by the groups of Korgel and Johnston^{67,73} using the high-temperature thermal decomposition of organosilane and organogermane compounds in supercritical alkanes in the presence of gold nanoparticles protected by a monolayer of an organic capping ligand such as an alkane-thiol. The process requires that the reaction temperature be higher than the eutectic temperature of the metal seed particle and the desired semiconductor, which is typically in excess of 350°C. For example, gold is used as the seed nanocrystal for Si wires, as gold and silicon are known to form an alloy containing 18.6% silicon at temperatures exceeding 363°C. In supercritical hexane at 500°C, the precursor readily decomposes on the gold surface and dissolves into the nanocrystal. It is then expelled from the crystal as a wire, which can exhibit growth from one lattice plane over larger distances, although twinning can also occur.⁷⁴ The use of a high-density SCF medium enables solvation of the precursor, stabilization of

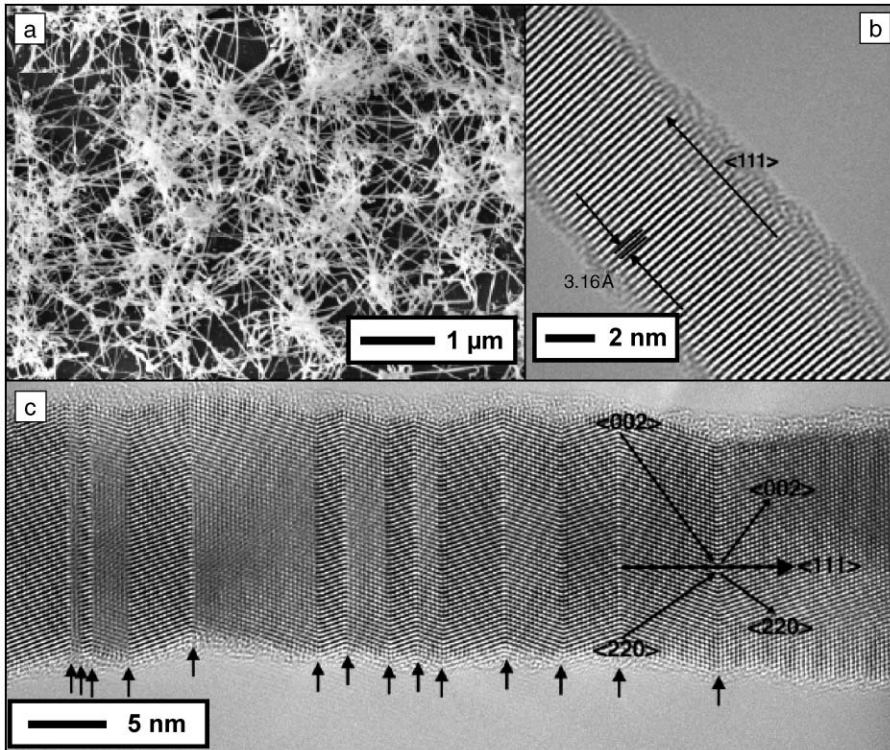


Figure 7. Gallium phosphide nanowires synthesized in supercritical fluids. (a) Scanning electron microscopy image of GaP nanowires grown at 500°C in hexane from (t-Bu)₃Ga and P(SiMe₃)₃. (b) High-resolution transmission electron microscopy (TEM) image of a GaP wire. (c) High-resolution TEM image of twinning faults in a GaP nanowire. Images reproduced with permission from Reference 75.

the seed particles prior to wire growth, and the high temperatures necessary for decomposition of the semiconductor particles in high yield. Several hydrocarbon fluids can be used at elevated temperatures before significant solvent degradation occurs (~600°C for toluene).⁷⁵ Davidson used a similar method to generate gallium phosphide wires and gallium arsenide wires at 500°C in hexane using t(Bu)₃Ga as the gallium source and P(SiMe₃)₃ and As(SiMe₃)₃, respectively (Figure 7).^{75,76}

Conclusions

Supercritical fluids offer a combination of properties that are uniquely suited for device fabrication at the nanoscale. The ability to conduct solution-based processing in an environment that, from a transport perspective, behaves more like a gas offers the possibility for extending deposition, cleaning, etching, and surface modification chemistries within the smallest device features envisioned by the semiconductor technology roadmaps. Conformal metal coverage via supercritical fluid deposition within challenging topographies offers a glimpse of this potential. We

expect SFD will be extended for metal oxide depositions in the near future. The synthesis of nanoparticles and nanowires in SCFs is developing rapidly and the approaches established to date offer promise for efficient production required for commercialization.

The 3D replication of pre-organized templates offers the potential for complete structural specification in next-generation device substrates. In addition to providing access to well-ordered nanoporous media through the use of block copolymers, the potential to create directly patterned media using templates prepared by nanoimprint lithography and other methods offers a significant reduction in process steps and thus economic as well as technical advantages. The ability to efficiently produce arrays of well-defined perpendicular nanochannels in silica and titania alone offers numerous possibilities for device fabrication in the areas of sensors, separation media, and energy conversion. Successful scaling of the 3D replication approach to robust ultralow-dielectric films containing spherical pores on 200-mm process wafers indicates the viability of these processes.

Acknowledgments

The authors gratefully acknowledge funding from the National Science Foundation through the NIRT (CTS 0304159), GOALI (CTS 0245002), and MRSEC (DMR 9400488) programs.

References

1. P.J. Linstrom and W.G. Mallard, eds., *NIST Chemistry WebBook, NIST Standard Reference Database Number 69* (National Institute of Standards and Technology, Gaithersburg, Md., June 2005); Web site <http://webbook.nist.gov> (accessed September 2005).
2. Y.F. Zong, PhD thesis, University of Massachusetts (2005).
3. B.D. Vogt, PhD thesis, University of Massachusetts (2003).
4. R.R. Gupta, V.S. RamachandraRao, and J.J. Watkins, *Macromolecules* **36** (2003) p. 1295.
5. *International Technology Roadmap for Semiconductors (ITRS), 2003 Edition*, <http://public.itrs.net/Files/2003ITRS/Home2003.htm> (accessed September 2005).
6. *International Technology Roadmap for Semiconductors (ITRS), 2004 Update*, <http://www.itrs.net/Common/2004Update/2004Update.htm> (accessed September 2005).
7. G.L. Weibel and C.K. Ober, *Microelectron. Eng.* **65** (2003) p. 145.
8. A. O'Neil and J.J. Watkins, *Green Chem.* **6** (2004) p. 363.
9. C.A. Jones, A. Zweber, J.P. DeYoung, J.B. McClain, R. Carbonell, and J.M. DeSimone, *Crit. Rev. Solid State Mater. Sci.* **29** (2004) p. 97.
10. F. Cansell, C. Aymonier, and A. Loppinet-Serani, *Curr. Opin. Solid State Mater. Sci.* **7** (2003) p. 331.
11. B.N. Hansen, B.M. Hybertson, R.M. Barkley, and R.E. Sievers, *Chem. Mater.* **4** (1992) p. 749.
12. R.E. Sievers and B.N. Hansen, "Chemical Deposition Methods Using Supercritical Fluid Solutions," U.S. Patent 4,970,093 (November 13, 1990).
13. V.K. Popov, V.N. Bagratashvili, E.N. Antonov, and D.A. Lemenovski, *Thin Solid Films* **279** (1996) p. 66.
14. J.M. Blackburn, D.P. Long, A. Cabanas, and J.J. Watkins, *Science* **294** (2001) p. 141.
15. A. Cabanas, X.Y. Shan, and J.J. Watkins, *Chem. Mater.* **15** (2003) p. 2910.
16. J.M. Blackburn, D.P. Long, and J.J. Watkins, *Chem. Mater.* **12** (2000) p. 2625.
17. E.T. Hunde and J.J. Watkins, *Chem. Mater.* **16** (2004) p. 498.
18. D.P. Long, J.M. Blackburn, and J.J. Watkins, *Adv. Mater.* **12** (2000) p. 913.
19. J.J. Watkins, J.M. Blackburn, and T.J. McCarthy, *Chem. Mater.* **11** (1999) p. 213.
20. A. Cabanas, D.P. Long, and J.J. Watkins, *Chem. Mater.* **16** (2004) p. 2028.
21. A. O'Neil and J.J. Watkins, (2005) unpublished manuscript.
22. E. Kondoh, *Jpn. J. Appl. Phys. Pt. 1: Regul. Pap. Short Notes Rev. Pap.* **43** (2004) p. 3928.
23. Y.F. Zong and J.J. Watkins, *Chem. Mater.* **17** (2005) p. 560.
24. Y.F. Zong, X.Y. Shan, and J.J. Watkins, *Langmuir* **20** (2004) p. 9210.

25. J.M. Blackburn, J. Gaynor, J. Drewery, E. Hundt, and J.J. Watkins, *Adv. Metallization Conf. Proc.* (Warrendale, PA, 2003) p. 601.
26. J.J. Watkins, J.M. Blackburn, D.P. Long, and J.L. Lazorcik, "Chemical Fluid Deposition Method for the Formation of Metal and Metal Alloy Films on Patterned and Unpatterned Substrates," U.S. Patent 6,689,700 (February 10, 2004).
27. J.J. Watkins and T.J. McCarthy, "A Method of Chemically Depositing Material onto a Substrate," U.S. Patent 5,789,027 (August 4, 1998).
28. H. Ohde, S. Kramer, S. Moore, and C.M. Wai, *Chem. Mater.* **16** (2004) p. 4028.
29. X.R. Ye, C.M. Wai, D.Q. Zhang, Y. Kranov, D.N. McLroy, Y.H. Lin, and M. Engelhard, *Chem. Mater.* **15** (2003) p. 83.
30. H. Wakayama, N. Setoyama, and Y. Fukushima, *Adv. Mater.* **15** (2003) p. 742.
31. B. Xie, C.C. Finstad, and A.J. Muscat, *Chem. Mater.* **17** (2005) p. 1753.
32. C.A. Bessel, G.M. Denison, J.M. DeSimone, J. DeYoung, S. Gross, C.K. Schauer, and P.M. Visintin, *J. Am. Chem. Soc.* **125** (2003) p. 4980.
33. X.Y. Shan and J.J. Watkins, *Thin Solid Films* (2005) in press.
34. C.T. Cao, A.Y. Fadeev, and T.J. McCarthy, *Langmuir* **17** (2001) p. 757.
35. J.R. Combes, L.D. White, and C.P. Tripp, *Langmuir* **15** (1999) p. 7870.
36. B.P. Gorman, R.A. Orozco-Teran, Z. Zhang, P.D. Matz, D.W. Mueller, and R.F. Reidy, *J. Vac. Sci. Technol. B* **22** (2004) p. 1210.
37. B. Xie and A.J. Muscat, in *Ultra-Clean Processing of Silicon Surfaces VII*, Vol. 103–104 (Trans Tech, Brussels, 2005) p. 323.
38. B. Xie and A.J. Muscat, *Microelectron. Eng.* **76** (2004) p. 52.
39. J.M. Cotte, D.L. Goldfarb, K.J. McCullough, W.M. Moreau, K.R. Pope, J.P. Simons, and C.J. Taft, "Process of Drying Semiconductor Wafers Using Liquid or Supercritical Carbon Dioxide," U.S. Patent 6,398,875 (June 4, 2002).
40. J.M. Cotte, D.L. Goldfarb, K.J. McCullough, W.M. Moreau, K.R. Pope, J.P. Simons, and C.J. Taft, "Process of Cleaning Semiconductor Processing, Handling, and Manufacturing Equipment," U.S. Patent 6,454,869 (September 24, 2002).
41. D.L. Goldfarb, J.J. de Pablo, P.F. Nealey, J.P. Simons, W.M. Moreau, and M. Angelopoulos, *J. Vac. Sci. Technol. B* **18** (2000) p. 3313.
42. H. Namatsu, *J. Photopolym. Sci. Technol.* **15** (2002) p. 381.
43. H. Namatsu, *Jpn. J. Appl. Phys. Pt. 2: Lett. Express Lett.* **43** (2004) p. L456.
44. H. Namatsu, K. Yamazaki, and K. Kurihara, *J. Vac. Sci. Technol. B* **18** (2000) p. 780.
45. E.N. Hoggan, D. Flowers, K. Wang, J.M. DeSimone, and R.G. Carbonell, *Ind. Eng. Chem. Res.* **43** (2004) p. 2113.
46. N. Sundararajan, S. Yang, K. Ogino, S. Valiyaveetil, J.G. Wang, X.Y. Zhou, C.K. Ober, S.K. Obendorf, and R.D. Allen, *Chem. Mater.* **12** (2000) p. 41.
47. V.Q. Pham, R.J. Ferris, A. Hamad, and C.K. Ober, *Chem. Mater.* **15** (2003) p. 4893.
48. D. Flowers, E.N. Hoggan, R. Carbonell, and J.M. DeSimone, *SPIE Proc.* **419** (2002) p. 4690.
49. F.S. Bates and G.H. Fredrickson, *Physics Today* **52** (1999) p. 32.
50. B.D. Vogt, G.D. Brown, V.S. Ramachandrarao, and J.J. Watkins, *Macromolecules* **32** (1999) p. 7907.
51. B.D. Vogt, V.S. Ramachandrarao, R.R. Gupta, K.A. Lavery, T.J. Francis, T.P. Russell, and J.J. Watkins, *Macromolecules* **36** (2003) p. 4029.
52. V.S. Ramachandrarao, R.R. Gupta, T.P. Russell, and J.J. Watkins, *Macromolecules* **34** (2001) p. 7923.
53. R.R. Gupta, K.A. Lavery, T.J. Francis, J.R.P. Webster, G.S. Smith, T.P. Russell, and J.J. Watkins, *Macromolecules* **36** (2003) p. 346.
54. R.G. Wissinger and M.E. Paulaitis, *J. Polym. Sci. Pt. B-Polym. Phys.* **25** (1987) p. 2497.
55. J.J. Watkins and T.J. McCarthy, *Macromolecules* **28** (1995) p. 4067.
56. J.J. Watkins and T.J. McCarthy, *Macromolecules* **27** (1994) p. 4845.
57. D.H. Sun, R. Zhang, Z.M. Liu, Y. Huang, Y. Wang, J. He, B.X. Han, and G.Y. Yang, *Macromolecules* **38** (2005) p. 5617.
58. J.J. Watkins and T.J. McCarthy, *Chem. Mater.* **7** (1995) p. 1991.
59. R.A. Pai, R. Humayun, M.T. Schulberg, A. Sengupta, J.N. Sun, and J.J. Watkins, *Science* **303** (2004) p. 507.
60. S. Nagarajan, R.A. Pai, T.P. Russell, J.J. Watkins, M. Li, K.S. Bosworth, P. Busch, D.M. Smilgies, and C.K. Ober, *Adv. Mater.* (2005) submitted.
61. P. Du, M.Q. Li, K. Douki, X.F. Li, C.R.W. Garcia, A. Jain, D.M. Smilgies, L.J. Fetters, S.M. Gruner, U. Wiesner, and C.K. Ober, *Adv. Mater.* **16** (2004) p. 953.
62. B.D. Vogt, R.A. Pai, H.J. Lee, R.C. Hedden, C.L. Soles, W.L. Wu, E.K. Lin, B.J. Bauer, and J.J. Watkins, *Chem. Mater.* **17** (2005) p. 1398.
63. R.A. Pai and J.J. Watkins, *Adv. Mater.* (2005) accepted.
64. W.E. Stallings and H.H. Lamb, *Langmuir* **19** (2003) p. 2989.
65. D.M. Hess and J.J. Watkins (2005) unpublished manuscript.
66. G. Bhatnagar and J.J. Watkins (2005) unpublished manuscript.
67. P.S. Shah, T. Hanrath, K.P. Johnston, and B.A. Korgel, *J. Phys. Chem. B* **108** (2004) p. 9574.
68. J.P. Cason, K. Khambaswadkar, and C.B. Roberts, *Ind. Eng. Chem. Res.* **39** (2000) p. 4749.
69. J.C. Liu, P. Raveendran, Z. Shervani, Y. Ikushima, and Y. Hakuta, *Chem. Eur. J.* **11** (2005) p. 1854.
70. C.L. Kitchens and C.B. Roberts, *Ind. Eng. Chem. Res.* **43** (2004) p. 6070.
71. H.L. Zhang, B.X. Han, J.C. Liu, X.G. Zhang, G.Y. Yang, and H.Z. Zhao, *J. Supercrit. Fluids* **30** (2004) p. 89.
72. M.C. McLeod, M. Anand, C.L. Kitchens, and C.B. Roberts, *Nano Lett.* **5** (2005) p. 461.
73. T. Hanrath and B.A. Korgel, *Adv. Mater.* **15** (2003) p. 437.
74. J.D. Holmes, K.P. Johnston, R.C. Doty, and B.A. Korgel, *Science* **287** (2000) p. 1471.
75. F.M. Davidson, R. Wiacek, and B.A. Korgel, *Chem. Mater.* **17** (2005) p. 230.
76. F.M. Davidson, A.D. Schrickler, R.J. Wiacek, and B.A. Korgel, *Adv. Mater.* **16** (2004) p. 646. □

Chapter Challenge ²⁰⁰⁶

—an event designed to spark a little
"friendly competition" among MRS Chapters.

The premise is simple. We've come up with a theme,

Biology—The Next Frontier of Materials Science and Engineering, and we want to see just what your members can do with it.

That's it. We're giving you the theme and not much more. Your challenge is to come up with a creative program or activity that relates to biology and materials science & engineering... and then make it happen!

Details for the competition can be found on our Web site: www.mrs.org/university/2006challenge

So get your Chapter together and set the creative juices flowing. It's a great way to energize your membership, increase student involvement, and showcase your Chapter.

Deadline for entries is **April 1, 2006**. The winning Chapter will be announced May 1, 2006 and will be featured in a summer issue of the *MRS Bulletin*.

Don't lose another minute. The Chapter **Challenge** starts NOW!